Degradation Of Humic Acids in Peat Water Using Fe_3O_4 Synthesized from Zircon Sand Tailing as Photo-Fenton Catalyst

Erwin Prasetya Toepak[1], Marvin Horale Pasaribu[1*], Retno Agnestisia[1], Gabriela Elsandika[2]

[1]Chemistry Department, Faculty of Mathematics and Natural Sciences, University of Palangka Raya, Palangka Raya 73111, Central Kalimantan, Indonesia

[2]Physics Department, Faculty of Mathematics and Natural Sciences, University of Palangka Raya, Palangka Raya 73111, Central Kalimantan, Indonesia

[*]Email: marvin.pasaribu@mipa.upr.ac.id

Received 28 November 2024
Accepted 28 March 2025
Published 30 June 2025

Abstract

Zircon sand mining generates significant magnetic waste, presenting an opportunity for valorization into valuable materials. This study explored the synthesis of Fe_3O_4 from zircon sand mining residues and its application as a photo-Fenton catalyst for humic acid degradation in peat water. Fe_3O_4 was synthesized via co-precipitation and characterized using FTIR and XRD, confirming the formation of a crystalline magnetite structure with distinct Fe–O bonding. Photocatalytic tests revealed an optimal catalyst mass of 0.03 g, achieving 87.06% humic acid degradation within 100 minutes under UV light with the addition of 1 mL H_2O_2. The photo-Fenton system exhibited high efficiency due to the generation of hydroxyl radicals (•OH), which facilitated the breakdown of complex organic molecules. Kinetic analysis indicated that the degradation followed a second-order reaction mechanism, with a rate constant of 8.29×10^{-4} M^{-1}•min^{-1} and an R^2 value of 0.9911. Excess catalyst mass reduced performance due to side reactions and turbidity effects. This study demonstrates that Fe_3O_4 derived from mining waste is an efficient and sustainable catalyst for addressing environmental challenges, particularly in treating humic acid-rich peat water, contributing to sustainable water management solutions.

Keywords: *Fe_3O_4 catalyst, humic acid, photo-fenton, zircon mining waste*

How to cite

Toepak, E.P., Pasaribu, M.H., Agnestisia, R., Elsandika, G. (2025). Degradation Of Humic Acids in Peat Water Using Fe_3O_4 Synthesized from Zircon Sand Tailing as Photo-Fenton Catalyst. *Jurnal Kimia Riset*, *10*(1), 1–16.

Highlights

1. Magnetite Fe_3O_4 was successfully synthesized from zircon sand mining waste via a co-precipitation method, as confirmed by crystalline magnetite through FTIR and XRD analysis.
2. As a photo-Fenton catalyst, Fe_3O_4 achieved 87.06% degradation of humic acid in peat water within 100 minutes using 0.03 g of catalyst and 1 mL of H_2O_2.
3. The degradation process followed second-order kinetics with a high correlation coefficient ($R^2 = 0.9911$), indicating efficient interaction between hydroxyl radicals and humic acid.
4. Excessive catalyst or H_2O_2 reduced degradation efficiency due to side reactions and limited UV light penetration caused by turbidity.
5. This study demonstrates the potential of valorizing zircon mining waste into sustainable catalytic materials for environmental water treatment applications.

Introduction

Peat water, commonly found in Indonesia's lowland regions such as Sumatra and Kalimantan, presents significant challenges for use as a clean water source due to its high levels of natural organic matter, primarily humic (HA) and fulvic acids (FA) (Qadafi et al., 2023). These compounds not only give umicpeat water its distinct brown coloration but also contribute to its acidic pH, requiring extensive treatment before it can be utilized for domestic or industrial purposes (Sativa et al., 2021). Several conventional treatment methods, including coagulation-flocculation, sedimentation, and membrane filtration, have been employed to purify peat water; however, their effectiveness in fully removing dissolved organic matter remains limited (Elma et al., 2021). Similarly, adsorption, filtration, and ozonation have shown limited efficacy, often failing to address the complex organic structure of humic substances (Qadafi et al., 2023; Sugandi et al., 2024). Emerging technologies, including advanced oxidation processes (AOPs), offer promising alternatives by employing reactive radicals to degrade persistent organic pollutants, including humic acids (HA).

Advanced Oxidation Processes (AOPs) represent a cutting-edge approach for addressing wastewater treatment challenges, particularly for the removal of persistent organic pollutants that resist conventional methods (Lama et al., 2022). These processes rely on the generation of hydroxyl radicals (•OH), highly reactive species capable of breaking down complex organic molecules into simpler, less harmful forms (Khan et al., 2023). AOPs are broadly categorized into homogeneous systems, which use soluble oxidants like hydrogen peroxide and ozone, and heterogeneous systems, which rely on solid-phase semiconductors as catalysts (Lama et al., 2022). Among the various AOPs, photocatalytic methods—combining UV or visible light with a catalyst—stand out for their versatility and efficiency in degrading pollutants like pharmaceuticals and dyes (Khader et al., 2024). The photo-Fenton process, a notable example, has demonstrated remarkable efficiency in degrading pharmaceutical compounds in effluents from wastewater treatment plants, achieving degradation rates as high as 71.9% to 100% (Napoleao et al., 2018). Beyond pollutant removal, AOPs also enhance the biodegradability and reduce the toxicity of wastewater, making them an indispensable tool for managing industrial and municipal wastewater sustainably (Khader et al., 2024). Photocatalysis is now recognized as one of the most efficient methods for treating peat water, driving research efforts toward the development of advanced semiconductor-based materials (Beladona et al., 2023).

Previous investigations have extensively examined the use of various metal oxide catalysts in the photodegradation of peat water, focusing on their ability to address its complex organic composition. Zinc oxide (ZnO) catalysts have demonstrated moderate efficiency in degrading humic acid (HA) through photosonolysis, achieving a degradation rate of up to 21.99% (Zulkarnaini et al., 2022). Titanium dioxide (TiO_2)-based catalysts, utilized both as slurries and as coatings on ceramic beads, have proven effective in reducing color intensity, chemical oxygen demand (COD), and humic acid (HA) concentration while simultaneously enhancing water conductivity. These improvements indicate TiO_2's potential for transforming the quality of peat water into a more usable form (Tanos et al., 2024). A particularly innovative approach using TiO_2-PP floating photocatalysts has shown significant success in removing humic acid and iron, with solar irradiation yielding superior results compared to UV lamp exposure (B. S. Nugroho et al.,

2023). However, the need for cost-effective and sustainable catalysts remains unmet. Magnetite (Fe_3O_4), with its unique magnetic separability, high surface area, and catalytic activity, has emerged as a promising candidate. Recent studies have highlighted its adaptability under both UV and visible light for degrading various pollutants, including methylene blue and industrial dyes (Pasaribu et al., 2024). However, its application in humic acid degradation within peat water remains underexplored.

Zircon sand ($ZrSiO_4$) is a valuable mineral widely used in industries such as ceramics and advanced materials. Indonesia contributes approximately 4% of the global zircon market, with Central Kalimantan holding significant reserves, estimated at over 5.4 billion tons (Suseno, 2015). Through processes like magnetic separation, acid leaching, and alkali fusion, the zirconium dioxide (ZrO_2) content in raw zircon sand can be increased from 42% to 66%, enhancing its industrial value (Murtadho et al., 2022). In addition to its benefits, zircon mining generates significant waste, particularly residues rich in magnetic minerals like magnetite (Fe_3O_4). These by-products, rather than being discarded, present opportunities for recovery and reuse in high-value applications, such as catalysis and environmental remediation. Utilizing these residues not only adds economic value but also mitigates environmental impacts, underscoring the importance of integrating resource efficiency and ecological sustainability in the extraction of zircon sand.

Magnetite (Fe_3O_4) is a versatile material with distinctive properties such as a high surface area, excellent magnetic separability, and robust catalytic activity, making it an exceptional candidate for environmental remediation (Agnestisia, 2017). Recent advancements in research have revealed its effectiveness as a photocatalyst for degrading a variety of organic pollutants, including industrial dyes. It is typically synthesized through methods like coprecipitation (Nengsih et al., 2024)These Fe_3O_4 are often derived from natural iron sources and exhibit soft magnetic properties. This unique characteristic allows these nanoparticles to be effortlessly separated from water after treatment, enabling practical and sustainable applications (Blanco-Gutiérrez et al., 2022). The photocatalytic performance of Fe_3O_4 is notable both under ultraviolet (UV) and visible light, showcasing its adaptability in diverse conditions. Studies have demonstrated its ability to effectively degrade persistent pollutants such as methylene blue and polyethylene terephthalate (PET) (Blanco-Gutiérrez et al., 2022; Nengsih et al., 2024). Moreover, combining Fe_3O_4 with complementary materials, such as titanium dioxide (TiO_2), silicon dioxide (SiO_2), or biopolymers like alginate, can significantly enhance its efficiency. These composites leverage synergistic effects to improve light absorption, pollutant interaction, and overall degradation rates, making Fe_3O_4 a promising material in advancing photocatalytic technologies for environmental cleanup (Nengsih et al., 2024; Wardhani et al., 2023).

In this study, Fe_3O_4 was synthesized from zircon sand mining waste, a by-product rich in magnetic minerals. This approach not only valorizes industrial waste but also aligns with the Sustainable Development Goals by minimizing environmental impacts. The research aims to evaluate the photocatalytic efficiency of Fe_3O_4 as a photo-Fenton catalyst, addressing the challenges of humic acid degradation in peat water. By comparing its performance to alternative methods, this study contributes to advancing sustainable water treatment technologies.

Research Methods

Materials

The magnetic waste was sourced from zircon sand mining in Kapuas Regency, peat water obtained from ponds in

Palangka Raya City, humic acid (HA) for standard (Aldrich technical grade), hydrochloric acid (HCl) 37% (Merck Pro Analysis), ammonia (NH_3) 25% (Merck Pro Analysis), hydrogen peroxide (H_2O_2) 30% (Merck Pro Analysis), and distilled water.

Instrumentation

The tools utilized included laboratory glassware (Pyrex), UV light box with LED UV lamp (365 nm, Epileds), external magnetic bar, Whatman Filter Paper, Analytical Balance (Ohaus PR224), centrifuge (Hettich EBA 200), Hotplate Stirrer (Thermo Scientific CH), oven (Memmert UN30), Orbital Shaker (Kang Jian), X-ray diffraction (XRD) (Philips with X'Pert MPD), and Fourier Transform Infrared Spectroscopy (FTIR) (Shimadzu FTIR-8400S spectrometer).

Procedure

1) Magnetic materials separation from zircon mining waste

   The magnetic material utilized for photocatalysis was derived from zircon sand waste through a systematic extraction process. Initially, the zircon sand waste underwent magnetic separation using an external magnet to isolate the magnetic components (Soylak et al., 2021). The isolated material was then ground manually with a mortar and pestle, followed by sieving with a 100-mesh sieve to achieve finer particle sizes.

2) Synthesis of magnetite (Fe_3O_4) from magnetic waste

   Preparation of magnetite (Fe_3O_4) was performed using a combined extraction and co-precipitation technique (Pasaribu et al., 2024). Initially, 6 g of magnetic waste was dissolved in 60 mL of concentrated hydrochloric acid (HCl) and stirred at 80 °C for 90 minutes until a greenish solution indicative of dissolved iron compounds was achieved. This solution was filtered twice to remove impurities. The filtrate was gradually titrated with 1 M ammonia hydroxide (NH_3) solution until the pH reached 9, prompting the formation of black Fe_3O_4 precipitate. The precipitate was then separated efficiently using an external magnetic field, ensuring the isolation of magnetically active particles. To remove residual impurities, the precipitate was thoroughly washed with distilled water until a neutral pH of 7 was achieved. Finally, the purified Fe_3O_4 was dried under controlled conditions in a vacuum oven at 60 °C for 12 hours.

3) Photo-fenton degradation of humic acid (HA) by Fe_3O_4

   The photocatalytic activity of Fe_3O_4 was evaluated using humic acid (HA) as a model organic pollutant. An amount of 0.03 g of Fe_3O_4 catalyst was introduced into 50 mL of peat water and stirred at 150 rpm under dark conditions for 120 minutes, with sampling every 20 minutes. Following the initial reaction phase, 1 mL of 30% hydrogen peroxide (H_2O_2) was added, initiating the photo-degradation process under UV irradiation at 365 nm. During this phase, samples were collected every 10 minutes for a total duration of 100 minutes to analyze the degradation process. To assess treatment efficiency, absorbance measurements were taken using a UV-Vis spectrophotometer at 354 nm before and after the degradation. Variations in experimental parameters, including Fe_3O_4 catalyst weight (0.02 g and 0.04 g) and H_2O_2 volume (0.5 mL and 1.5 mL), were tested to examine their influence on photocatalytic performance.

   The optimal dosage of Fe_3O_4 catalyst and H_2O_2 is determined by evaluating the highest removal efficiency percentage (%), which is calculated using Equation (1). Here, A_o represents the absorbance of peat water before the degradation process,

while A_t indicates the absorbance after the degradation process.

$$\% \text{ Degradation} = \frac{(A_o - A_t)}{(A_o)} \times 100 \qquad (1)$$

Results and Discussion

Magnetic separation is an effective technique for isolating valuable minerals from waste materials in mining operations. This process exploits differences in magnetic properties of various minerals, separating them based on their magnetic susceptibility (Herrera-Pérez et al., 2023). In zircon sand ($ZrSiO_4$) mining, magnetic waste often contains iron-rich minerals like magnetite (Fe_3O_4), ilmenite ($FeTiO_3$), and hematite (Fe_2O_3). By utilizing a combination of magnetic separation and co-precipitation, the extraction efficiency of Fe_3O_4 was enhanced, with yields exceeding 85% under optimal conditions (Khuzaima et al., 2018; Moscoso-Pinto & Kim, 2021). High-purity Fe3O4 can be obtained from iron sand through a process involving magnetic separation, acid dissolution, and precipitation, resulting in a single-phase product with ferromagnetic properties (Gunanto et al., 2018). These findings support the feasibility of processing magnetic waste to recover Fe_3O_4 efficiently.

The synthesis of Fe_3O_4 involves three main steps: leaching, alkaline precipitation, and the formation of Fe_3O_4 (Pasaribu et al., 2024). The magnetic fraction from the waste is extracted with HCl, producing Fe^{2+} and Fe^{3+} ions, which are subsequently titrated with NH_4OH to reach pH 9 to form a mixture of iron hydroxides (Kristina et al., 2024) as described in Equations (2) to (6).

$$Fe_2O_{3\,(s)} + 6HCl\,(aq) \rightarrow 2Fe^{+3}\,(aq) + 3H_2O \qquad (2)$$

$$Fe_3O_4\,(s) + 8HCl\,(aq) \rightarrow Fe^{+2}\,(aq) + 2Fe^{+3}\,(aq) + 4H_2O \qquad (3)$$

$$Fe^{+3}\,(aq) + 3\,OH^{-}\,(aq) \rightarrow Fe(OH)_3\,(s) \qquad (4)$$

$$Fe^{+3}\,(aq) + 2\,OH^{-}\,(aq) \rightarrow Fe(OH)_2\,(s) \qquad (5)$$

$$Fe(OH)_2\,(s) + 2Fe(OH)_3\,(s) \rightarrow Fe_3O_4\,(s) + 4H_2O \qquad (6)$$

The process continues with heating at approximately 60 °C, where $Fe(OH)_2$ and $Fe(OH)_3$ react to form Fe_3O_4 and water. The resulting black Fe_3O_4 precipitate, which exhibits magnetic properties and a crystalline magnetite structure, is then washed with distilled water to remove residual ions, such as Na^+ and Cl^-, and dried to eliminate remaining moisture. The final product demonstrates its magnetic response to an external magnetic field, as shown in Figure 1, showcasing the potential of transforming industrial waste into valuable materials for purification technology applications.

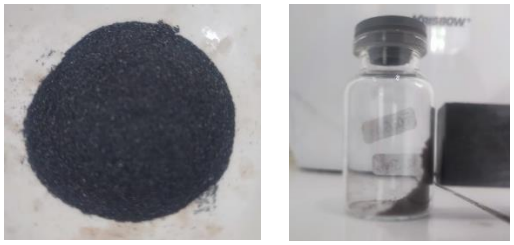

(a) (b)

Figure 1. (a) Fe_3O_4 material, (b) magnetic properties test to an external magnetic field

The FTIR spectrum of the synthesized Fe_3O_4 material, presented in Figure 2, spans the wavenumber range of 400–4000 cm^{-1}. The spectrum exhibits characteristic peaks indicating the presence of Fe–O bonds in octahedral and tetrahedral positions. Absorption peaks observed at

537 cm^{-1} and 419 cm^{-1} correspond to the stretching vibrations of Fe–O bonds at these positions (Agnestisia, 2017). These features confirm the successful synthesis of magnetite (Fe_3O_4) with magnetic properties derived from the arrangement of Fe^{2+} and Fe^{3+} ions in octahedral and tetrahedral sites within its crystal lattice (Husain et al., 2019). This structure plays a crucial role in supporting the functionality of Fe_3O_4 as a catalyst in photo-Fenton reactions. The magnetic and electronic properties of Fe_3O_4 enable efficient electron transfer, which is a key mechanism in catalytic photo-Fenton reactions.

Additionally, the FTIR spectrum of Fe_3O_4 shows no absorption peaks in the range of 3000–3500 cm^{-1}, which typically indicates hydroxyl (–OH) groups from adsorbed water. The absence of these peaks suggests that the synthesized magnetite is relatively free from water or hydroxyl groups, reflecting an efficient synthesis and drying process. These findings align with previous studies, which reported such peaks due to environmental moisture or water used during synthesis (Villegas et al., 2020).

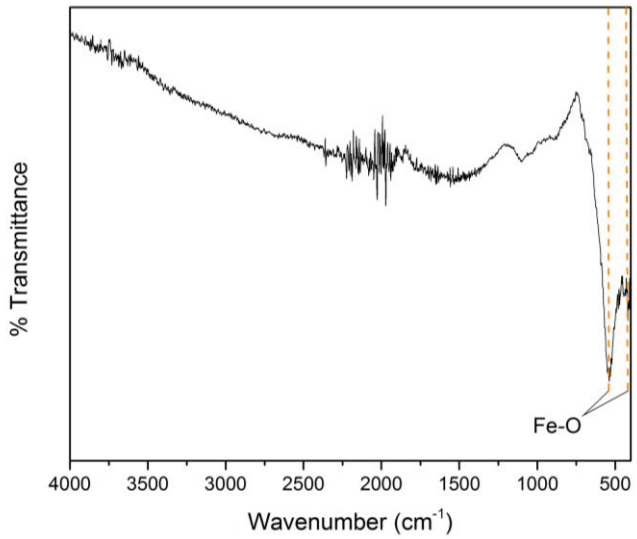

Figure 2. FTIR spectra of Fe_3O_4

The XRD analysis of the magnetite Fe_3O_4 material is presented in Figure 3. The X-ray diffraction (XRD) pattern of the synthesized Fe_3O_4 reveals four prominent diffraction peaks at 2θ angles of 30.20°, 35.43°, 43.05°, and 56.88°. According to the Joint Committee on Powder Diffraction Standards (JCPDS No. 19-0629), these peaks correspond to the *hkl* of (220), (311), (400), and (511) crystal planes, respectively. These peaks are characteristic of the spinel structure of magnetite (Fe_3O_4) (Budi et al., 2019). This diffraction pattern confirms that the synthesized material exhibits an ordered crystal structure with a magnetite phase, essential for catalytic applications. The spinel structure provides a stable configuration of Fe^{2+} and Fe^{3+} ions within the crystal lattice, ensuring material stability in chemical reactions (Saragi et al., 2018).

The crystallinity of Fe_3O_4, as evidenced by the sharp peaks in the XRD pattern, plays a crucial role in its effectiveness as a catalyst in photo-fenton reactions. The well-ordered crystal structure enables efficient electron transfer between Fe^{2+} and Fe^{3+} during catalytic processes. This electron transfer facilitates the generation of highly reactive hydroxyl radicals (•OH), which degrade complex organic compounds in water into simpler molecules (M. G.

Nugroho et al., 2024). Furthermore, the magnetite phase identified in the XRD pattern highlights the magnetic properties of Fe_3O_4, allowing easy separation of the catalyst from the reaction solution using an external magnetic field. This feature enhances process efficiency and promotes sustainability, as the catalyst can be reused without leaving residues in the solution (Gadgeel et al., 2019).

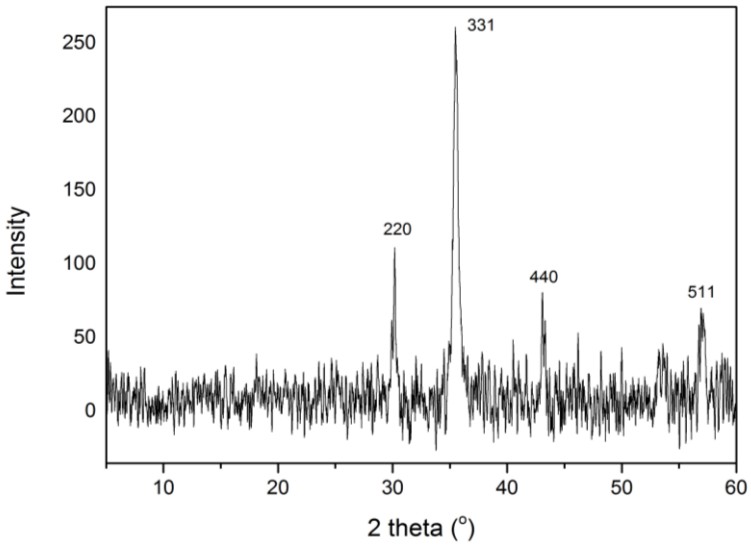

Figure 3. XRD diffractograms of Fe_3O_4

The photocatalytic degradation test of humic acid was conducted to evaluate the performance of Fe_3O_4 as a catalyst in the photo-Fenton system. Initially, adsorption was performed in dark conditions to ensure equilibrium, which is crucial for assessing the material's intrinsic adsorption capacity. Subsequently, the system was exposed to UV radiation to initiate the photo-Fenton reaction. The effect of varying Fe_3O_4 catalyst masses (0.02 g, 0.03 g, and 0.04 g) on humic acid degradation was evaluated.

As shown in Figure 4a, the results under dark conditions revealed low degradation levels, with the highest value being 13.32% for 0.03 g. UV exposure significantly enhanced degradation. At 10 minutes, degradation reached approximately 55% across all Fe_3O_4 mass variations, with 0.03 g demonstrating the highest efficiency. This emphasizes the crucial role of UV-activated H_2O_2 in generating hydroxyl radicals (•OH), which act as the primary agents driving the degradation process (Liu et al., 2021). However, increasing the mass from 0.03 g to 0.04 g reduced efficiency, indicating an optimal catalyst mass.

The highest degradation of humic acid was observed with 0.03 g of catalyst (87.06%) at 100 minutes, while 0.04 g showed reduced performance due to side reactions that decreased the concentration of effective hydroxyl radicals and generated less reactive radicals such as $•HO_2$ (Karim et al., 2021). The reduced efficiency with excessive Fe_3O_4 (0.04 g) is attributed to factors such as side reactions among radicals, the precipitation of $Fe(OH)_3$, which hinders the regeneration of Fe^{2+} and Fe^{3+} ions, and blocks the diffusion of radicals to humic acid molecules. Additionally, excessive catalyst mass increased solution turbidity, reducing UV light penetration and the activation of H_2O_2 (Wang et al., 2023). These combined factors resulted in lower degradation efficiency, highlighting the importance of optimizing the catalyst quantity in the photo-Fenton reaction. The change in color of peat water resulting from the photo-Fenton degradation of humic acid is presented in Figure 5b.

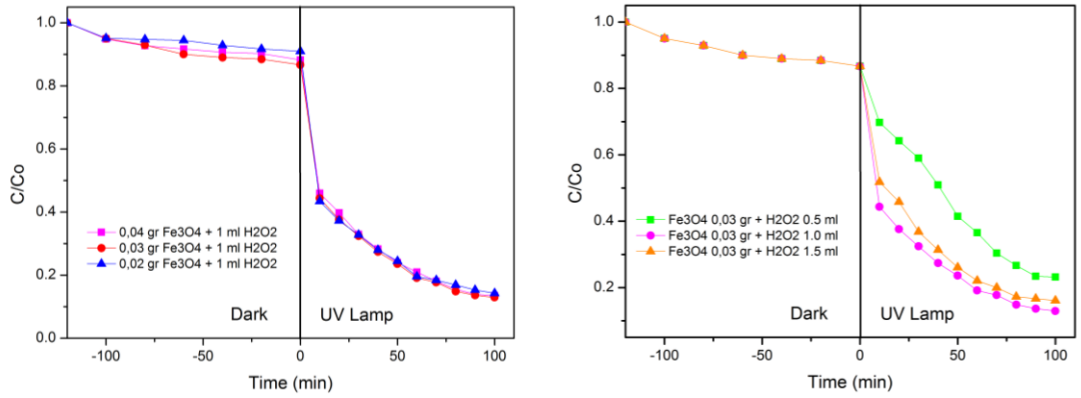

(a) (b)

Figure 4. Photo-Fenton degradation of HA activity curves with different weights of (a) Fe_3O_4 catalyst, (b) volume of H_2O_2

As illustrated in Figure 4b, the photo-fenton system exhibited varying degrees of humic acid degradation when subjected to different volumes of hydrogen peroxide (H_2O_2). Upon initiation of UV irradiation at the zero-minute mark, a substantial acceleration in humic acid degradation was observed. At the 10-minute interval, degradation percentages reached 30.2%, 55.7%, and 48.2% for H_2O_2 volumes of 0.5 mL, 1.0 mL, and 1.5 mL, respectively. This enhancement underscores the role of UV light in activating H_2O_2 to produce highly reactive hydroxyl radicals (•OH), which effectively dismantle the intricate organic structure of humic acid (Sun et al., 2024). Among the tested volumes, 1.0 mL emerged as the optimal dosage, yielding the highest degradation. Interestingly, further increasing the H_2O_2 concentration did not proportionally improve degradation efficiency, likely due to competing side reactions (Ramos et al., 2020).

Humic acid degradation had progressed to 76.84%, 87.06%, and 84.03% at 100 minutes for the 0.5 mL, 1.0 mL, and 1.5 mL H_2O_2 volumes, respectively. The decreased efficiency at 1.5 ml is attributed to side reactions, such as the formation of hydroperoxyl radicals ($•HO_2$), which are less reactive than hydroxyl radicals. These side reactions reduce the effective radicals available for degradation (Shen et al., 2020). Additionally, excess H_2O_2 can lead to an accumulation of Fe^{3+} ions, which inhibits the regeneration of Fe^{2+} in the Fenton cycle, ultimately lowering the production of hydroxyl radicals (Zhou et al., 2017).

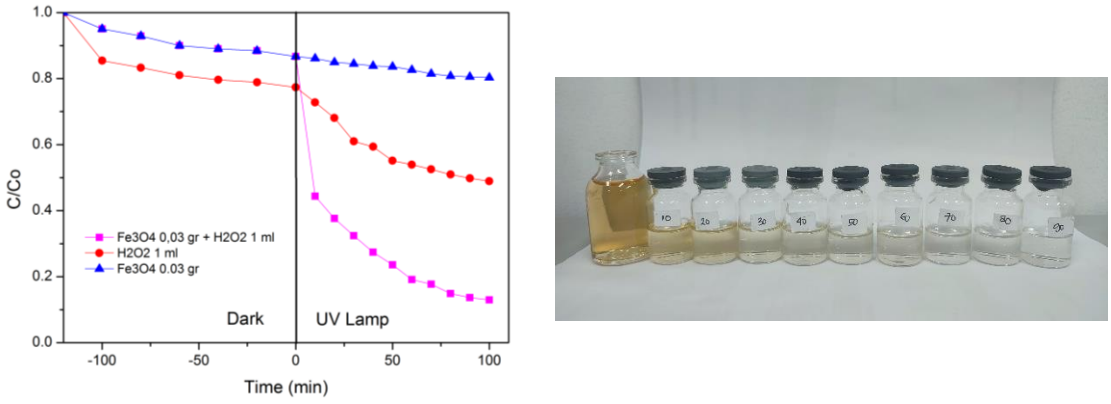

(a) (b)

Figure 5. Photo-Fenton degradation activity curves of HA with different condition (a); and colour change of HA degradation (b)

Figure 5a demonstrates that photodegradation of humic acid is influenced by the roles of Fe_3O_4, H_2O_2, and their combination under both dark conditions and UV exposure. In the dark, oxidative activity remains minimal due to the limited formation of hydroxyl radicals (•OH), which are the primary oxidants in this process. H_2O_2 exhibits slight oxidative activity even without UV, while Fe_3O_4 acts as a passive catalyst. The combination of Fe_3O_4 and H_2O_2 shows no significant improvement in the absence of UV light, as degradation reactions are not yet optimal without UV activation. UV exposure significantly enhances photodegradation efficiency, particularly for the Fe_3O_4 and H_2O_2 combination. In contrast, Fe_3O_4 or H_2O_2 alone exhibits much lower degradation efficiency, highlighting the importance of their combined interaction in the photodegradation of humic acid. The subsequent Fenton process generates hydroxyl radicals (•OH), which are further enhanced by UV light to degrade organic compounds into degraded products (Mahmud et al., 2021). The underlying reaction mechanism is provided in Equations (7) to (10).

$$Fe_3O_4 + H^+ \rightarrow Fe^{2+} + Fe^{3+} + H_2O \quad (7)$$

$$Fe^{2+} + H_2O_2 \rightarrow Fe^{3+} + HO^- + \bullet OH \quad (8)$$

$$Fe^{3+} + H_2O_2 \rightarrow Fe^{2+} + H^+ + \bullet HO_2 \quad (9)$$

$$\bullet OH + HA \rightarrow \text{Degraded HA products} \quad (10)$$

Table 1. Performance comparison of the Fe_3O_4 catalyst with other recently reported catalysts for the degradation of humic acid (HA):

Catalyst	Dosage	Time	Efficiency	Reference
α-Fe_2O_3/NiS_2	0.1 g/L	100 min	93.7 %	(Mohtar et al., 2021)
Ag-WO3/bentonite	100 mg	360 min	91 %	(Ajel & Al-nayili, 2022)
Ag-TiO_2/HAP/Al_2O_3	15 mg/L	60 min	88.3 %	(Ma et al., 2010)
Fe_3O_4	30 mg	100 min	87.06 %	This work
$FeSO_4 \cdot 7H_2O$	10^{-5} mol.L^{-1}	120 min	78 %	(Katsumata et al., 2008)
TiO_2/Cu-areca fiber	30 mg	180 min	54 %	(Sugandi et al., 2024)
ZnO	30 mg	120 min	21.99 %	(Zulkarnaini et al., 2022)

Based on Table 1, the Fe_3O_4 catalyst developed in this study demonstrated 87.06% efficiency in degrading humic acid (HA) within 100 minutes, placing it among the more effective options. Although α-Fe_2O_3/NiS_2 (93.7%) and Ag-WO_3/bentonite (91%) showed slightly better results, Fe_3O_4 outperformed several other catalysts, including $FeSO_4 \cdot 7H_2O$ (78%), TiO_2/Cu-areca fiber (54%), and ZnO (21.99%). With its high effectiveness and reasonable reaction time, Fe_3O_4 presents strong potential for further enhancement, particularly through modifications aimed at improving its photocatalytic capabilities.

The catalytic kinetics model of the Photo-Fenton process was employed to analyze the degradation of humic acid and measure its reaction rate. Both first-order and second-order kinetics were evaluated using ln (Co/C) versus time for first-order, and 1/C versus time for second-order models as shown in Figure 6a-b.

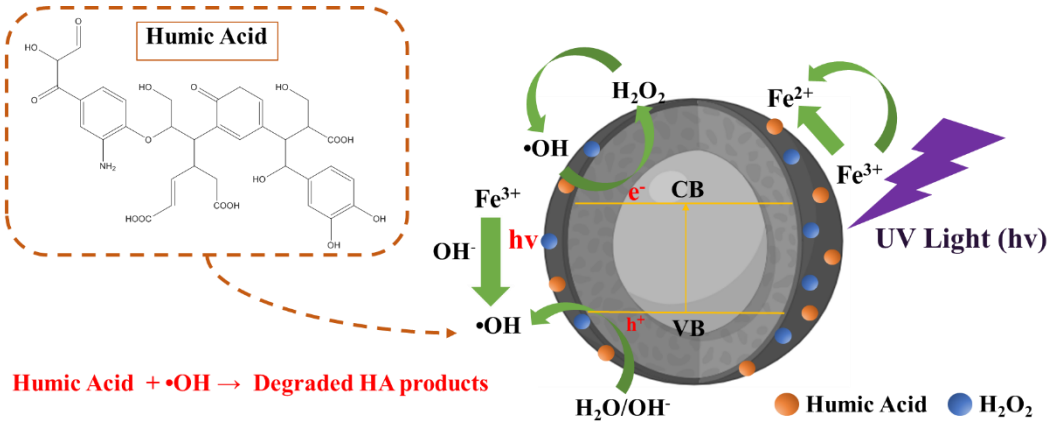

Figure 6. Cycle of Humic Acid Degradation via Fe_3O_4 Fenton Catalyst

Figure 7 and Table 2 revealed that R^2 values for the first-order model across various conditions—such as H_2O_2 (UV), Fe_3O_4 (UV), and Fe_3O_4 combined with H_2O_2—ranged from 0.8942 to 0.9837, indicating moderate correlation but incomplete adherence to first-order kinetics. In contrast, the second-order model showed higher R^2 values, ranging from 0.9608 to 0.9917, suggesting a better fit and implying that the degradation process of humic acid by Fe_3O_4 likely follows second-order kinetics, where the reaction rate strongly depends on the interaction between hydroxyl radicals (•OH) and humic acid molecules. This kinetic model is consistent with the previous study (Wu et al., 2010). The analysis supports the second-order kinetic mechanism, where the degradation rate increases with the concentration of radicals produced. The highest reaction rate constant (k) was recorded at 8.29×10^{-4} M^{-1}. min^{-1} for 0.03 g of Fe_3O_4, indicating that this amount of catalyst is optimal for accelerating humic acid degradation. However, at 0.04 g of Fe_3O_4, the reaction rate constant decreased slightly, suggesting a saturation effect or side reactions caused by the excess catalyst. This highlights the importance of optimizing catalyst quantity to achieve maximum degradation efficiency in the photo-fenton reaction.

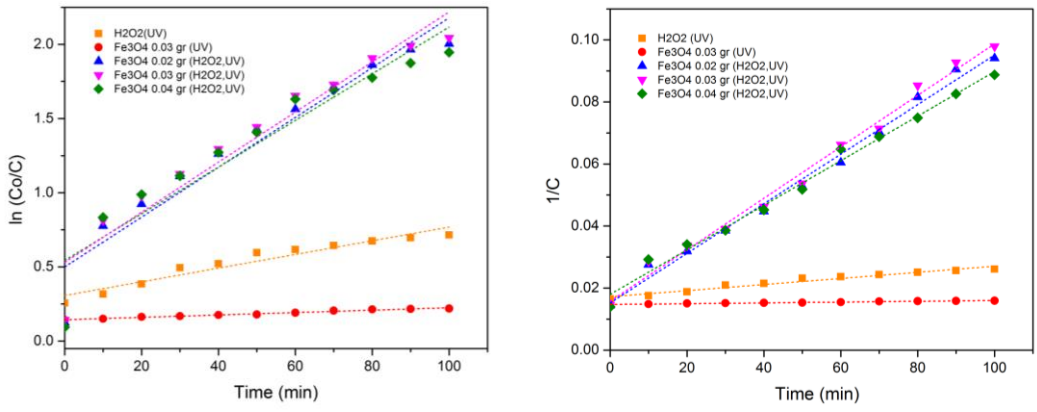

(a) (b)

Figure 7. First-order (a); and second-order (b) kinetic model graphics of photo-fenton degradation of HA under various conditions

Table 2. Parameters of the first-order and second-order photo-fenton degradation kinetics model under different conditions

Material and condition	First-order		Second-order	
	R^2	k_1 (min^{-1})	R^2	k_2 ($M^{-1}.min^{-1}$)
H_2O_2 (UV)	0.9379	4.61×10^{-3}	0.9608	1.02×10^{-4}
Fe_3O_4 0.03 g (UV)	0.9837	8.03×10^{-4}	0.9793	1.33×10^{-5}
Fe_3O_4 0.02 g (H_2O_2, UV)	0.9325	1.67×10^{-2}	0.9917	7.98×10^{-4}
Fe_3O_4 0.03 g (H_2O_2, UV)	0.9281	1.70×10^{-2}	0.9911	8.29×10^{-4}
Fe_3O_4 0.04 g (H_2O_2, UV)	0.8942	1.57×10^{-2}	0.9898	7.18×10^{-4}

Conclusions

This study successfully synthesized Fe_3O_4 magnetite from zircon mining waste, demonstrating its superior performance as a photo-Fenton catalyst for humic acid degradation in peat water. Characterization confirmed the successful synthesis, with FTIR identifying Fe–O bonds at wavenumbers 537 cm^{-1} and 419 cm^{-1}, and supported by analysis of XRD indicating crystallinity at 2θ angles of 30.14°, 35.51°, 43.19°, and 56.96°. In photocatalytic activity, Fe_3O_4 at a mass of 0.03 g achieved the highest humic acid degradation efficiency of 87.06% within 100 minutes under UV light with the addition of 1 ml of H_2O_2. This enhanced performance is attributed to the semiconductor properties of Fe_3O_4, which facilitate the formation of hydroxyl radicals. Kinetic analysis revealed a second-order reaction, with Fe_3O_4 (0.03 g) + 1 ml H_2O_2 exhibiting the highest rate constant (8.29×10^{-4} $M^{-1}.min^{-1}$) with an R^2 value of 0.9911. These findings highlight the potential of Fe_3O_4 magnetite as an effective and sustainable catalyst for wastewater treatment applications.

Author Contributions

EPT and **MHP** conceptualized and designed the research framework. **EPT** conducted the synthesis and characterization of Fe_3O_4. **RA** carried out the photo-Fenton degradation experiments and collected the data. GE performed data analysis and contributed to data visualization. **MHP** and **EPT** wrote the original draft. **MHP** and **RA** revised and edited the manuscript. **MHP** and **GE** supervised the project and managed the research administration. All authors contributed to the discussion and approved the final version of the manuscript.

Conflict of Interest

The authors have declared that there is no conflict of interest.

Acknowledgment

The authors would like to acknowledge the University of Palangka Raya for providing essential laboratory facilities and infrastructure to support this research. The authors also express their sincere gratitude to the zircon sand mining company in Kapuas Regency for generously supplying the sample materials used in this study.

Funding

This research was funded by the University of Palangka Raya through a research grant awarded in 2024, under contract number 2224/UN.24.13/AL.04/2024.

References

Agnestisia, R. (2017). Synthesis & Characterization of Magnetit (Fe3O4) and Its Applications as Adsorbent Methylene Blue. *Jurnal Sains Dan Terapan Kimia*, *11*(2), 61. https://doi.org/10.20527/jstk.v11i2.4039

Ajel, M. K., & Al-nayili, A. (2022). Synthesis, characterization of Ag-WO3/bentonite nanocomposites and their application in photocatalytic degradation of humic acid in water. *Environmental Science and Pollution Research*, *30*(8), 20775–20789. https://doi.org/10.1007/s11356-022-23614-4

Beladona, S. U. M., Putra, R., Alfanaar, R., Sylvani, M. M., Alyatikah, E., Safitri, R., Susanti, I., & Iqbal, R. M. (2023). A Review: Development of Photocatalyst Materials and Its Performance for Humic Acid Removal in Peatwater. *Journal of Peat Science and Innovation*, *1*(1), 1–15. https://doi.org/10.59032/jpsi.v1i1.5380

Blanco-Gutiérrez, V., Li, P., Berzal-Cabetas, R., & Dos santos-García, A. J. (2022). Exploring the photocatalytic activity of nanometric magnetite for PET materials degradation under UV light. *Journal of Solid State Chemistry*, *316*, 123509. https://doi.org/10.1016/j.jssc.2022.123509

Budi, H., Husain, H., Supanun, L., & Suminar, P. (2019). Examination of Natural and Standard Fe3O4 Powders Using X-Ray Absorption Near-Edge Spectroscopy (XANES). *Materials Science Forum*, *964*, 40–44. https://doi.org/10.4028/www.scientific.net/MSF.964.40

Elma, M., Pratiwi, A. E., Rahma, A., Rampun, E. L. A., Mahmud, M., Abdi, C., Rosadi, R., Yanto, D. H. Y., & Roil, M. (2021). Combination of Coagulation, Adsorption, and Ultrafiltration Processes for Organic Matter Removal from Peat Water. *Sustainability*, *14*(1), 370. https://doi.org/10.3390/su14010370

Gadgeel, A. A., Mhaske, S. T., Duerr, C., & Liu, K. L. (2019). In-Situ Preparation and Characterization of Aconitic Acid Capped Fe3O4 Nanoparticle by Using Citric Acid as a Reducing Agent. *Journal of Inorganic and Organometallic Polymers and Materials*, *29*(5), 1688–1700. https://doi.org/10.1007/s10904-019-01131-1

Gunanto, Y. E., Izaak, M. P., Jobiliong, E., Cahyadi, L., & Adi, W. A. (2018). High purity Fe_3O_4 from Local Iron Sand Extraction. *Journal of Physics: Conference Series*, *1011*, 012005. https://doi.org/10.1088/1742-6596/1011/1/012005

Herrera-Pérez, J. G., Legorreta-García, F., Reyes-Pérez, M., Reyes-Cruz, V. E., Chávez-Urbiola, E. A., & Trujillo-Villanueva, L. E. (2023). Analysis of the Effect of Magnetic Separation Processing Parameters for the Treatment of Mining Waste. *Polish Journal of Environmental Studies*. https://doi.org/10.15244/pjoes/173113

Husain, S., Irfansyah, M., Haryanti, N. H., Suryajaya, S., Arjo, S., & Maddu, A. (2019). Synthesis and characterization of Fe3O4 magnetic nanoparticles from iron ore. *Journal of Physics: Conference Series*, *1242*(1), 012021. https://doi.org/10.1088/1742-6596/1242/1/012021

Karim, M. A. H., Aziz, K. H. H., Omer, K. M., Salih, Y. M., Mustafa, F., Rahman, K. O., & Mohammad, Y. (2021). Degradation of aqueous organic dye pollutants by heterogeneous photo-assisted Fenton-like process using natural

mineral activator: Parameter optimization and degradation kinetics. *IOP Conference Series: Earth and Environmental Science*, *958*(1), 012011. https://doi.org/10.1088/1755-1315/958/1/012011

Katsumata, H., Sada, M., Kaneco, S., Suzuki, T., Ohta, K., & Yobiko, Y. (2008). Humic acid degradation in aqueous solution by the photo-Fenton process. *Chemical Engineering Journal*, *137*(2), 225–230. https://doi.org/10.1016/j.cej.2007.04.019

Khader, E. H., Muslim, S. A., Saady, N. M. C., Ali, N. S., Salih, I. K., Mohammed, T. J., Albayati, T. M., & Zendehboudi, S. (2024). Recent advances in photocatalytic advanced oxidation processes for organic compound degradation: A review. *Desalination and Water Treatment*, *318*, 100384. https://doi.org/10.1016/j.dwt.2024.100384

Khan, Z. U. H., Gul, N. S., Sabahat, S., Sun, J., Tahir, K., Shah, N. S., Muhammad, N., Rahim, A., Imran, M., Iqbal, J., Khan, T. M., Khasim, S., Farooq, U., & Wu, J. (2023). Removal of organic pollutants through hydroxyl radical-based advanced oxidation processes. *Ecotoxicology and Environmental Safety*, *267*, 115564. https://doi.org/10.1016/j.ecoenv.2023.115564

Khuzaima, N., Ahmad, K. R., Ahmad Zaidi, N. H., Hashim, M. K. R., & Rezan, S. A. (2018). Minerals Characterization of Magnetic and Non-Magnetic Element from Black Sand Langkawi. *Solid State Phenomena*, *280*, 440–447. https://doi.org/10.4028/www.scientific.net/SSP.280.440

Kristina, N. P. D., Arjana, I. G., & Yasa, P. (2024). Synthesis And Characterization Of Magnetite Nanomaterials in Tianyar Iron Sand Using Co-Precipitation Method. *Indonesian Physical Review*, *7*(3), 398–413. https://doi.org/10.29303/ipr.v7i3.328

Lama, G., Meijide, J., Sanromán, A., & Pazos, M. (2022). Heterogeneous Advanced Oxidation Processes: Current Approaches for Wastewater Treatment. *Catalysts*, *12*(3), 344. https://doi.org/10.3390/catal12030344

Liu, Y., Zhao, Y., & Wang, J. (2021). Fenton/Fenton-like processes with in-situ production of hydrogen peroxide/hydroxyl radical for degradation of emerging contaminants: Advances and prospects. *Journal of Hazardous Materials*, *404*, 124191. https://doi.org/10.1016/j.jhazmat.2020.124191

Ma, N., Zhang, Y., Quan, X., Fan, X., & Zhao, H. (2010). Performing a microfiltration integrated with photocatalysis using an Ag-TiO2/HAP/Al2O3 composite membrane for water treatment: Evaluating effectiveness for humic acid removal and anti-fouling properties. *Water Research*, *44*(20), 6104–6114. https://doi.org/10.1016/j.watres.2010.06.068

Mahmud, N., Benamor, A., Nasser, M. S., Ba-Abbad, M. M., El-Naas, M. H., & Mohammad, A. W. (2021). Effective Heterogeneous Fenton-Like degradation of Malachite Green Dye Using the Core-Shell Fe3O4@SiO2 Nano-Catalyst. *ChemistrySelect*, *6*(4), 865–875. https://doi.org/10.1002/slct.202003937

Mohtar, S. S., Aziz, F., Nor, A. R. M., Mohammed, A. M., Mhamad, S. A., Jaafar, J., Yusof, N., Salleh, W. N. W., & Ismail, A. F. (2021). Photocatalytic degradation of humic acid using a novel visible-light active

α-Fe2O3/NiS2 composite photocatalyst. *Journal of Environmental Chemical Engineering*, *9*(4), 105682. https://doi.org/10.1016/j.jece.2021.105682

Moscoso-Pinto, F., & Kim, H.-S. (2021). Concentration and Recovery of Valuable Heavy Minerals from Dredged Fine Aggregate Waste. *Minerals*, *11*(1), 49. https://doi.org/10.3390/min11010049

Murtadho, I., Muslih, E. Y., & Kusuma, D. Y. (2022). *Zirconia content enrichment of Indonesian zircon sand by using alkali fusion followed by water leaching and sulfuric acid leaching*. 030006. https://doi.org/10.1063/5.0075013

Napoleao, D. C., Zaida, L. E. M. C., Rodríguez-Díaz, J. M., Santana, R. M. da R., Montenegro, M. C. B. da S. de M., Araújo, A. da N., Benachour, M., & Silva, V. L. da. (2018). Use of the photo-Fenton process to discover the degradation of drugs present in water from the Wastewater Treatment Plants of the pharmaceutical industry. *Journal of Chemical Engineering Theoretical and Applied Chemistry*, *75*(581).

Nengsih, S., Nur Abdulmadjid, S., Mursal, M., & Jalil, Z. (2024). Photocatalytic performance of Fe3O4-TiO2 in the degradation of methylene blue dye: Optimizing the usability of natural iron sand. *Materials Science for Energy Technologies*, *7*, 374–380. https://doi.org/10.1016/j.mset.2024.06.001

Nugroho, B. S., Asri, A., & Arman, Y. (2023). Exploring TiO2-PP as a Reusable Floating Photocatalyst for Humic Acid and Iron Removal in Peat Water. *Indonesian Journal Of Applied Physics*, *13*(2), 171. https://doi.org/10.13057/ijap.v13i2.60342

Nugroho, M. G., Putri, B. L. P., Mukharomah, N. L. A., Wibisono, A. A., Nurherdiana, S. D., & Wafi, A. (2024). Environmentally Friendly Bifunctional Materials Based On ZnO/Natural Zeolite for Methylene Blue Dye Removal in Water. *Jurnal Kimia Riset*, *9*(2), 210–224. https://doi.org/10.20473/jkr.v9i2.65751

Pasaribu, M. H., Karelius, K., Agnestisia, R., Toepak, E. P., & Pereiz, Z. (2024). Potential Of Magnetite (Fe_3O_4) Synthesized from Zircon Sand Waste As Methylen Blue Dye Adsorbent. *Jurnal Inovasi Teknik Kimia*, *9*(2), 98–107. https://doi.org/10.31942/inteka.v9i2.10112

Qadafi, M., Wulan, D. R., Notodarmojo, S., & Zevi, Y. (2023). Characteristics and treatment methods for peat water as clean water sources: A mini review. *Water Cycle*, *4*, 60–69. https://doi.org/10.1016/j.watcyc.2023.02.005

Ramos, R. O., Albuquerque, M. V. C., Lopes, W. S., Sousa, J. T., & Leite, V. D. (2020). Degradation of indigo carmine by photo-Fenton, Fenton, H2O2/UV-C and direct UV-C: Comparison of pathways, products and kinetics. *Journal of Water Process Engineering*, *37*(May), 101535. https://doi.org/10.1016/j.jwpe.2020.101535

Saragi, T., Permana, B., Saputri, M., Safriani, L., Rahayu, I., & Risdiana. (2018). Karakteristik Optik dan Kristal Nanopartikel Magnetit. *Jurnal Ilmu Dan Inovasi Fisika*, *2*(1), 53–56. https://doi.org/10.24198/jiif.v2i1.15438

Sativa, S. O., Zulfikar, M. A., Suryandari, E. T., & Nasir, M. (2021). Effect of Composite Composition in Nanofiber for Degradation of Humic Acid Solution. *Advanced Materials*

Research, *1162*, 87–92. https://doi.org/10.4028/www.scientific.net/AMR.1162.87

Shen, J.-H., Chuang, H.-Y., Jiang, Z.-W., Liu, X.-Z., & Horng, J.-J. (2020). Novel quantification of formation trend and reaction efficiency of hydroxyl radicals for investigating photocatalytic mechanism of Fe-doped TiO2 during UV and visible light-induced degradation of acid orange 7. *Chemosphere*, *251*, 126380. https://doi.org/10.1016/j.chemosphere.2020.126380

Soylak, M., Ozalp, O., & Uzcan, F. (2021). Magnetic nanomaterials for the removal, separation and preconcentration of organic and inorganic pollutants at trace levels and their practical applications: A review. *Trends in Environmental Analytical Chemistry*, *29*, e00109. https://doi.org/10.1016/j.teac.2020.e00109

Sugandi, D., Agustiawan, D., Wijayanto, E., Marpaung, M. O. P., Ayyash, M. Y., & Wahyuni, N. (2024). Degradation Of Humic Acid By Floating Photocatalyst TiO2/Cu-Areca Fiber. *Jurnal Kimia Riset*, *9*(1), 10–19. https://doi.org/10.20473/jkr.v9i1.50850

Sun, T., Jin, Z.-Y., Deng, B., He, G., Wang, Q.-Y., Hu, M., Han, Z., Zheng, Z., Zhao, J., Yun, J., Zhao, J., Zhu, Y., Pan, Z., Li, X., & Hu, Z.-T. (2024). Visible-light-driven photo-Fenton oxidation enhanced by Fe/Bi-nanocrystal phase transformation as a universal way for various organic pollutants mineralization. *Chemical Engineering Journal*, *481*, 148732. https://doi.org/10.1016/j.cej.2024.148732

Suseno, T. (2015). Analisis prospek pasir zirkon Indonesia di pasar dunia. *Jurnal Teknologi Mineral Dan Batubara*, *11*(1), 61–77.

Tanos, F., Razzouk, A., Lesage, G., Cretin, M., & Bechelany, M. (2024). A Comprehensive Review on Modification of Titanium Dioxide-Based Catalysts in Advanced Oxidation Processes for Water Treatment. *ChemSusChem*, *17*(6). https://doi.org/10.1002/cssc.202301139

Villegas, A. R., Ramírez, V. I. D. L., Guevara, J. H., Sicairos, E. P., Ayala, S. A. H., Sanchez, L. L., & Bertha. (2020). Synthesis and characterization of magnetite nanoparticles for photocatalysis of nitrobenzene. *Journal of Saudi Chemical Society*, *24*(2), 223–235. https://doi.org/10.1016/j.jscs.2019.12.004

Wang, Z., Jia, X., Sun, W., Wang, J., Li, C., Zhao, Q., Li, Y., & Tian, S. (2023). Persulfate-based remediation of organic-contaminated soil: Insight into the impacts of natural iron ions and humic acids with complexation/redox functionality. *Science of The Total Environment*, *905*, 167177. https://doi.org/10.1016/j.scitotenv.2023.167177

Wardhani, S., Mardiansyah, H. A., & Purwonugroho, D. (2023). Fe3O4-SiO2-Alginate Photocatalyst for Textile Dyes Waste Degradation. *Science and Technology Indonesia*, *8*(1), 108–115. https://doi.org/10.26554/sti.2023.8.1.108-115

Wu, Y., Zhou, S., Qin, F., Zheng, K., & Ye, X. (2010). Modeling the oxidation kinetics of Fenton's process on the degradation of humic acid. *Journal of Hazardous Materials*, *179*(1–3), 533–539. https://doi.org/10.1016/j.jhazmat.2010.03.036

Zhou, W., Gao, J., Zhao, H., Meng, X., & Wu, S. (2017). The role of quinone cycle in Fe2+ – H2O2 system in the regeneration of Fe2+. *Environmental*

Technology, *38*(15), 1887–1896. https://doi.org/10.1080/09593330.2016.1240241

Zulkarnaini, A., Sanjaya, H., Yohandri, Y., & Nizar, U. K. (2022). Degradasi Asam Humat Pada Air Rawa Gambut menggunakan Metode Fotosonolisis dengan Bantuan Katalis ZnO. *Jurnal Periodic Jurusan Kimia UNP*, *11*(1), 35. https://doi.org/10.24036/p.v11i1.113433